Simple model of bouncing ball dynamics: displacement of the table assumed as quadratic function of time

Andrzej Okninski[1], Bogusław Radziszewski[2]
Physics Division[1], Department of Mechatronics and Mechanical Engineering[2],
Politechnika Swietokrzyska, Al. 1000-lecia PP 7,
25-314 Kielce, Poland

October 15, 2010

Abstract

Nonlinear dynamics of a bouncing ball moving in gravitational field and colliding with a moving limiter is considered. Displacement of the limiter is a quadratic function of time. Several dynamical modes, such as fixed points, 2 - cycles and chaotic bands are studied analytically and numerically. It is shown that chaotic bands appear due to homoclinic structures created from unstable 2 - cycles in a corner-type bifurcation.

1 Introduction

Vibro-impacting systems belong to a very interesting and important class of nonsmooth and nonlinear dynamical systems [1, 2, 3, 4] with important technological applications [5, 6, 7, 8]. Dynamics of such systems can be extremely complicated due to velocity discontinuity arising upon impacts. A very characteristic feature of such systems is the presence of nonstandard bifurcations such as border-collisions and grazing impacts which often lead to complex chaotic motions.

The Poincaré map, describing evolution from an impact to the next impact, is a natural tool to study vibro-impacting systems. The main difficulty with investigating impacting systems is in finding instant of the next impact what typically involves solving a nonlinear equation. However, the problem can be simplified in the case of a bouncing ball dynamics assuming a special motion of the limiter. Bouncing ball models have been extensively studied, see [9] and references therein. As a motivation that inspired this work, we mention study of physics and transport of granular matter [6]. A similar model has been also used to describe the motion of railway bogies [7].

Recently, we have considered several models of motion of a material point in a gravitational field colliding with a limiter moving with piecewise constant velocity [10, 11, 12, 13, 14]. Moreover, we have proposed more realistic yet still simple models approximating sinusoidal motion of the table as exactly as possible but still preserving possibility of analytical compuations [15]. In the present work we study the model in which displacement of the table is a quadratic and periodic function of time.

The paper is organized as follows. In Section 2 a one dimensional dynamics of a ball moving in a gravitational field and colliding with a table is reviewed and the corresponding Poincare map is constructed. A bifurcation diagram is computed for displacement of the table assumed as quadratic and periodic function of time. In the next Section dynamical modes shown in the bifurcation diagram such as fixed points, 2 - cycles and chaotic bands are studied analytically and numerically. It is shown that chaotic bands appear due to homoclinic structures created from unstable 2 - cycles in a corner-type bifurcation. We summarize our results in Section 4.

2 Bouncing ball: a simple motion of the table

We consider a motion of a small ball moving vertically in a gravitational field and colliding with a moving table, representing unilateral constraints. The ball is treated as a material point while the limiter's mass is assumed so large that its motion is not affected at impacts. A motion of the ball between impacts is described by the Newton's law of motion:

$$m\ddot{x} = -mg, \tag{1}$$

where $\dot{x} = dx/dt$ and motion of the limiter is:

$$y = y(t), \tag{2}$$

with a known function y. We shall also assume that y is a continuous function of time. Impacts are modeled as follows:

$$x(\tau_i) = y(\tau_i), \tag{3}$$

$$\dot{x}\left(\tau_i^+\right) - \dot{y}(\tau_i) = -R\left(\dot{x}\left(\tau_i^-\right) - \dot{y}(\tau_i)\right), \tag{4}$$

where duration of an impact is neglected with respect to time of motion between impacts. In Eqs. (3), (4) τ_i stands for time of the i-th impact while $\dot{x}_i^-$, $\dot{x}_i^+$are left-sided and right-sided limits of $\dot{x}_i(t)$ for $t \to \tau_i$, respectively, and R is the coefficient of restitution, $0 \leq R < 1$ [5].

Solving Eq. (1) and applying impact conditions (3), (4) we derive the Poincaré map [16]:

$$\gamma Y(T_{i+1}) = \gamma Y(T_i) - \Delta_{i+1}^2 + \Delta_{i+1} V_i, \tag{5a}$$

$$V_{i+1} = -RV_i + 2R\Delta_{i+1} + \gamma(1+R)\dot{Y}(T_{i+1}), \tag{5b}$$

where $\Delta_{i+1} \equiv T_{i+1} - T_i$. The limiter's motion has been typically assumed in form $Y_s(T) = \sin(T)$, cf. [11] and references therein. This choice leads to serious difficulties in solving the first of Eqs.(5) for T_{i+1}, thus making analytical investigations of dynamics hardly possible. Accordingly, we have decided to simplify the limiter's periodic motion to make (5a) solvable.

In our previous papers we have assumed displacement of the table as piecewise linear periodic function of time [11, 12, 14]. In our recent work preliminary results for function $Y(T)$ assumed as quadratic Y_q and two cubic functions of time, Y_{c_1} and Y_{c_2} have been obtained [15]. In this work we study dynamics for quadratic function of time $Y_q(T)$:

$$Y_q(T) = \begin{cases} -16\hat{T}\left(\hat{T} - \frac{1}{2}\right), & 0 \le \hat{T} < \frac{1}{2} \\ 16\left(\hat{T} - \frac{1}{2}\right)\left(\hat{T} - 1\right), & \frac{1}{2} \le \hat{T} \le 1 \end{cases} \tag{6}$$

with $\hat{T} = T - \lfloor T \rfloor$, where $\lfloor x \rfloor$ is the floor function – the largest integer less than or equal to x, in more detail.

Since the period of motion of the limiter is equal to one, the map (5) is invariant under the translation $T_i \to T_i + 1$. Accordingly, all impact times T_i can be reduced to the unit interval $[0,\ 1]$. The model consists thus of equations (5), (6) with control parameters R, γ.

In Fig. 1 below we show the bifurcation diagram with times of impacts computed for growing γ and $R = 0.85$ (see also [15] where bifurcation diagram with velocities just after impacts against γ was shown).

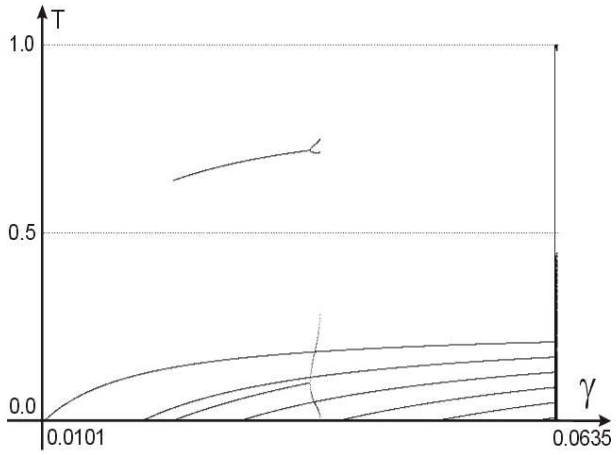

Figure 1: Bifurcation diagram. $R = 0.85$, $\gamma \in [0.0101,\ 0.0635]$.

It follows that dynamical system (5), (6) has several attractors: six fixed points, one 2 - cycle and, possibly, chaotic attractor.

3 Analytical results

We shall investigate now fixed points, 2 - cycle and chaotic bands shown in Fig. 1, combining analytical and numerical approach.

3.1 Fixed points

We shall first study periodic solutions with one impact per k periods. Such states have to fulfill the following conditions:

$$V_{n+1} = V_n \equiv V_*^{(k/1)},\ T_{n+1} = T_n + k \equiv T_*^{(k/1)} + k \qquad (k = 1, 2, \ldots), \tag{7}$$

where:

$$T_*^{(k/1)} \in (0,\ 1),\ V_*^{(k/1)} > \gamma \dot{Y}_q\left(T\right). \tag{8}$$

Substituting these conditions into (5), (6) we obtain two sets of fixed points:

$$\begin{aligned} 0 &\leq T_*^{(s)} = \tfrac{1}{4} - \tfrac{k(1-R)}{32\gamma(1+R)} \leq \tfrac{1}{2} \\ V_* &= k \end{aligned} \tag{9}$$

where the impact occurs in time interval $T_*^{(s)} \in \left(0,\ \frac{1}{2}\right)$ and

$$\begin{aligned} \tfrac{1}{2} &\leq T_*^{(u)} = \tfrac{3}{4} + \tfrac{k(1-R)}{32\gamma(1+R)} \leq 1 \\ V_* &= k \end{aligned} \tag{10}$$

with impacts taking place in time interval $T_*^{(u)} \in \left(\frac{1}{2},\ 1\right)$.

Solutions (9) fulfill physical requirements and are stable in the following interval of γ:

$$k\tfrac{1-R}{8(1+R)} \leq \gamma \leq \tfrac{1+R^2}{8(1+R)^2}, \tag{11}$$

where lower bound is a consequence of $T_*^{(s)} \geq 0$ while the upper bound follows from the condition that eigenvalues λ of the stability matrix obey $|\lambda| < 1$. On the other hand, solutions (10) are always unstable and are physical for:

$$\gamma \geq k\tfrac{1-R}{8(1+R)}, \tag{12}$$

what is equivalent to the condition $T_*^{(u)} \leq 1$.

3.2 2 - cycle

It follows from the bifurcation diagram, Fig. 1, that there exists a stable 2 - cycle with time of first impact $T_{*1} \in \left(0,\ \frac{1}{2}\right)$ and time of the second impact $T_{*2} \in \left(\frac{1}{2},\ 1\right)$. Such periodic solution must fulfill the following equations which

are easily obtained from Eqs. (5), (6):

$$\left\{\begin{array}{l} 16\gamma\left(T_{*2}-\frac{1}{2}\right)\left(T_{*2}-1\right)= \\ -16\gamma T_{*1}\left(T_{*1}-\frac{1}{2}\right)-\left(T_{*2}-T_{*1}\right)^{2}+\left(T_{*2}-T_{*1}\right)V_{*1} \\ V_{*2}=-RV_{*1}+2R\left(T_{*2}-T_{*1}\right)+\gamma\left(1+R\right)\left(32T_{*2}-24\right) \\ -16\gamma\left(T_{*3}-1\right)\left(\left(T_{*3}-1\right)-\frac{1}{2}\right)= \\ 16\gamma\left(T_{*2}-\frac{1}{2}\right)\left(T_{*2}-1\right)-\left(T_{*3}-T_{*2}\right)^{2}+\left(T_{*3}-T_{*2}\right)V_{*2} \\ V_{*3}=-RV_{*2}+2R\left(T_{*3}-T_{*2}\right)+\gamma\left(1+R\right)\left(8-32\left(T_{*3}-1\right)\right) \\ T_{*3}=T_{*1}+1 \\ V_{*3}=V_{*1} \end{array}\right. . \qquad (13)$$

Eliminating variables we arrive at equation for time of the first impact only:

$$C_4x^4+C_3x^3+C_2x^2+C_1x+C_0=0, \qquad (14)$$

where $x\equiv T_{1*}$ and

$$\left\{\begin{array}{l} C_0=\left(\left(8\gamma+1\right)R^2-8\gamma+1\right)\frac{\left(24\gamma+128\gamma^2+1\right)R^3+\left(384\gamma^2+8\gamma-1\right)R^2+\left(384\gamma^2-24\gamma+1\right)R+128\gamma^2-8\gamma-1}{\left(R+1\right)^3\left(R-1\right)^2} \\ C_1=-64\gamma\frac{\left(24\gamma+128\gamma^2+1\right)R^4-2R^3+\left(-512\gamma^2+2+32\gamma\right)R^2+\left(-2-512\gamma^2+64\gamma\right)R-128\gamma^2+8\gamma+1}{\left(R-1\right)^2\left(R+1\right)^2} \\ C_2=-2048\gamma^2\frac{-R^3+(-1+48\gamma)R^2+(-5+48\gamma)R+1}{\left(R-1\right)^2\left(R+1\right)} \\ C_3=4096\gamma^2\left(-1+16\gamma\right)\frac{R^2+2R-1}{\left(R-1\right)^2} \\ C_4=-4096\gamma^2\left(-1+16\gamma\right)\frac{R+1}{R-1} \end{array}\right. . \qquad (15)$$

It follows from the bifurcation diagram that the 2 - cycle is born when $T_1=x=0$. This in turn occurs when $C_0=0$. Equation $C_0=0$ has three roots:

$$\begin{array}{rcl} \gamma_1 & = & \frac{1}{8}\frac{1+R^2}{1-R^2}, \\ \gamma_2 & = & \frac{1}{32(R+1)}\frac{-3R^2+2R+1-\sqrt{R^4-12R^3-2R^2+4R+9}}{R+1}, \\ \gamma_3 & = & \frac{1}{32(R+1)}\frac{-3R^2+2R+1+\sqrt{R^4-12R^3-2R^2+4R+9}}{R+1}. \end{array} \qquad (16)$$

Testing Eqs. (16) against numerical computations we find out that the stable 2 - cycle is born at $\gamma=\gamma_3$. For example, for $R=0.85$ we have $\gamma_3=0.023\,367\,4$, cf. Fig 1.

3.3 Chaotic bands and homoclinic structure

Magnification of the bifurcation diagram near the origin of chaotic bands is shown in Fig. 2 below.

There are six chaotic bands (and six basins of attraction) above the critical point γ_{cr}. The first band which appears for appropriate initial conditions is shown in Fig. 3. Each band consists of two subbands only since due to cyclic periodic conditions points $T=0$, $T=1$ are identified.

We note that there is a switch of stability - fixed points become unstable precisely at $\gamma=\gamma_{cr}$ when chaotic bands appear. Then at $\gamma=\gamma_{cr}$ a homoclinic

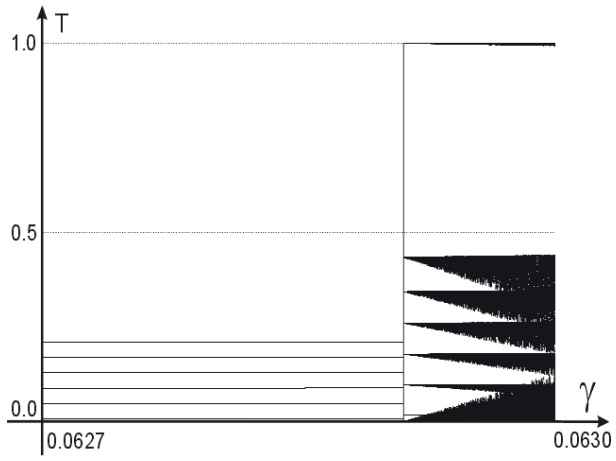

Figure 2: Bifurcation diagram. Six chaotic bands, $R = 0.85$, $\gamma \in [0.0627,\ 0.0630]$.

trajectory with $T = 1^-$ is probably created - this is suggested by presence of clusters of points near $T = 0$, $T = 1$. Computer simulations show that near γ_{cr} there are six unstable 2 - cycles. For $\gamma < \gamma_{cr}$ impacts occur in the following time intervals $T_{*1} \in \left(0,\ \frac{1}{2}\right), T_{*2} \in \left(1,\ 1\frac{1}{2}\right), T_{*3} \in \left(2+m,\ 2+m+\frac{1}{2}\right)$, $m = 0, 1, 2, \ldots$, and $T_{*3} = T_{*1} \mod 1$ where true impact times without cyclic conditions are shown. Then at $\gamma = \gamma_{cr}$ a corner event occurs, i.e. $T_{*2} = 1$. Indeed, at $T_{*2} = 1$ acceleration of the table is discontinuous. Then, for $\gamma > \gamma_{cr}$ another six unstable 2 - cycles are created with impact times $T_{*1} \in \left(0,\ \frac{1}{2}\right)$, $T_{*2} \in \left(\frac{1}{2},\ 1\right), T_{*3} \in \left(2+m,\ 2+m+\frac{1}{2}\right), m = 0.1.2.\ldots$, and $T_{*3} = T_{*1} \mod 1$.

It is now possible to write down equations, suggested by numerical computations, for the unstable 2 - cycles for $\gamma \geq \gamma_{cr}$:

$$\left\{\begin{array}{c} 16\gamma\left(y_m - \frac{1}{2}\right)(y_m - 1) = -16\gamma x\left(x - \frac{1}{2}\right) - (y-x)^2 + (y-x)\,u \\ v = -Ru + 2R\,(y-x) + \gamma\,(1+R)\,(32y_m - 24) \\ -16\gamma z_n\left(z_n - \frac{1}{2}\right) = 16\gamma\left(y_m - \frac{1}{2}\right)(y_m - 1) - (z-y_m)^2 + (z-y_m)\,v \\ w = -Rv + 2R\,(z-y_m) + \gamma\,(1+R)\,(8 - 32z_n) \\ z_n = x \\ w = u \end{array}\right. \tag{17}$$

where

$$\begin{array}{rcl} x & = & T_{*1},\ y = T_{*2},\ z = T_{*3}, \\ y_m & = & T_{*2} - m,\ z_n = T_{*3} - n, \\ u & = & V_{*1},\ v = V_{*2},\ w = V_{*3}, \end{array} \tag{18}$$

with integer m, n where numerical computations suggest that $n = m + 2$.

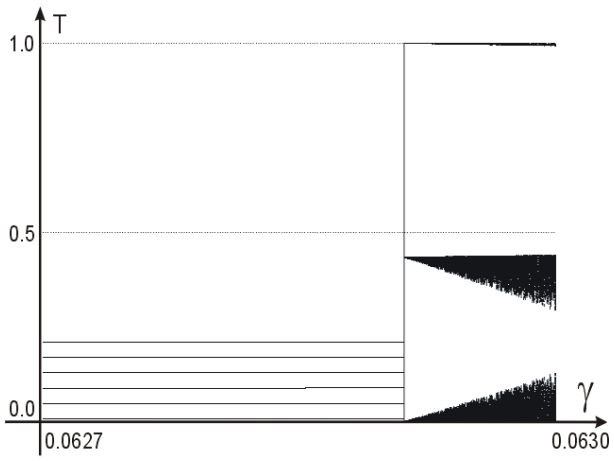

Figure 3: Bifurcation diagram. First chaotic band, $R = 0.85$, $\gamma \in [0.0627,\ 0.0630]$.

We are going to solve equations (17), (18) at $\gamma = \gamma_{cr}$ and this means that we have to put $y_m = 1$. It follows that there are six unstable 2 - cycles in question which are obtained for $m = 0, 1, \ldots, 5$ and $n = m + 2$, solutions for larger m's being nonphysical. Solving these equations we get:

$$\gamma_{cr} = \frac{1+R^2}{8(1+R)^2}, \quad n = m + 2, \tag{19}$$

$$T^{(cr)}_{*1,\,m} \equiv x = \frac{2R^2-6-4m+2\sqrt{(3+5m+2m^2)R^4+1+3m+2m^2}}{2(R^2-1)} - m - 2, \tag{20}$$

and we do not show more complicated expressions for $T^{(cr)}_{*2}$, $V^{(cr)}_{*1}$, $V^{(cr)}_{*2}$.

It follows from Eq. (20) that for $R = 0.85$ there are only six acceptable solutions with $T_{*1} > 0$ corresponding to six chaotic bands in Fig. 2. In the Table 1 impact times and the corresponding velocities just after the impact, computed from Eqs. (17), (19), (20), are listed for $R = 0.85$ and $m = 0, 1, \ldots, 5$:

Table 1

m	0	1	2	3	4	5
$T^{(cr)}_{*1,\,m}$	0.434 7	0.343 6	0.260 2	0.178 4	0.097 4	0.016 7
$V^{(cr)}_{*1,\,m}$	0.514 8	1.623 7	2.716 9	3.806 5	4.894 6	5.981 9
$T^{(cr)}_{*2,\,m}$	1^-	1^-	1^-	1^-	1^-	1^-
$V^{(cr)}_{*2,\,m}$	1.454 6	2.366 7	3.279 4	4.192 3	5.105 1	6.018 0

Critical 2 - cycle $m = 0$, $n = 2$ ($R = 0.85$) is shown below.

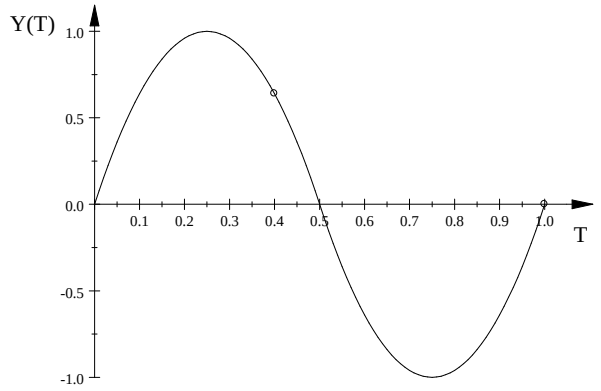

Figure 4: Critical 2 - cycle. Position of the 2 - cycle is denoted by open circles.

In Figs. 5, 6 the second chaotic band and first two chaotic bands are shown. The bifurcation diagrams for $\gamma > \gamma_{cr} = 0.06291\ldots$ were computed for initial conditions shown in the Table 1.

Sharp edges of chaotic bands are given within good approximation by $T^{(cr)}_{*1,\,m}$ and also $T = 0, 1$. It seems that the homoclinic structure exists for all values of $\gamma > \gamma_{cr}$ shown in the Figures.

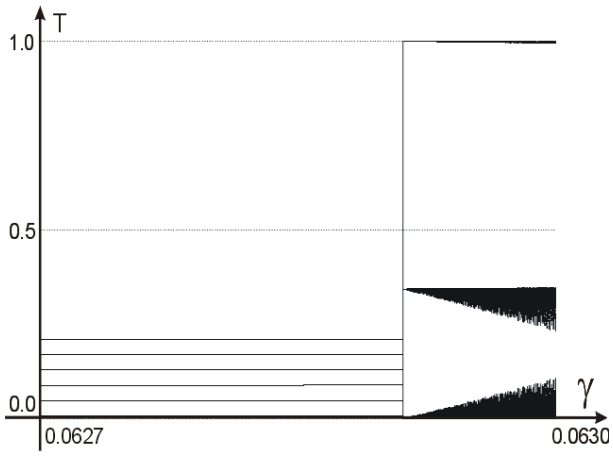

Figure 5: Bifurcation diagram. Second chaotic band, $R = 0.85$, $\gamma \in [0.0627,\ 0.0630]$.

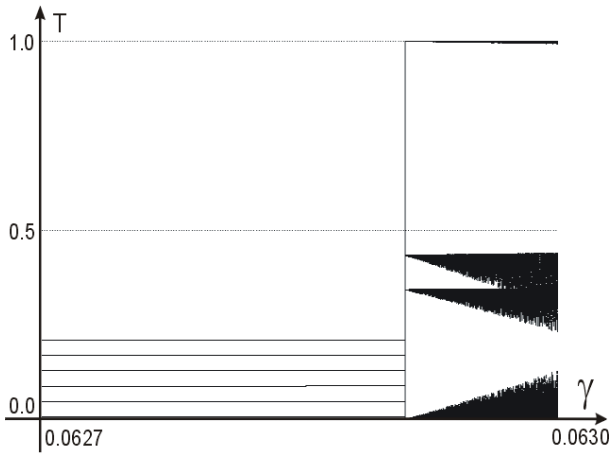

Figure 6: Bifurcation diagram. First two chaotic bands, $R = 0.85$, $\gamma \in [0.0627,\ 0.0630]$.

We have also computed Lyapunov exponents, cf. the Table 2.

Table 2

m	0	1	2	3	4	5
λ_m	0.2	1.2	1.6	1.85	2.0	2.1

4 Discussion and closing remarks

We have studied dynamics of a material point moving vertically in a gravitational field and colliding with a limiter. Displacement of the limiter has been assumed as quadratic function of time (6). Due to the simplicity of the problem it was possible to investigate the dynamics analytically with some support from numerical computations. Firstly, fixed points were found and their stability was determined. Secondly, equations for a stable 2 - cycle were found and simplified, cf. Eqs. (14), (15). From these equations analytical condition for birth of the 2 - cycle was found (cf. $\gamma = \gamma_3$ in Eq.(16)). Finally, a transition to chaotic dynamics was described in analytical terms. It was shown that six stable chaotic bands appear from six unstable 2 - cycles. Equations for these 2 - cycles were found and solved to yield critical value of γ, Eq. (19), and impact times and the corresponding velocities at $\gamma = \gamma_{cr}$, see Eq. (20) where $T^{(cr)}_{*1,\ m}$ was given. Approximation to the band edges was also found.

We have demonstrated, combining analytical and numerical approach, that at the transition point $\gamma = \gamma_{cr}$ unstable 2 - cycles give rise to homoclinic structures which lead to chaotic behaviour. This transition is a corner-type bifurcation similar to that found in a bouncing ball model with piecewise linear velocity [14]. In our future work we shall study models with displacement of the table described by a cubic functions of time [15].

References

[1] M. di Bernardo, C.J. Budd, A.R. Champneys, P. Kowalczyk, *Piecewise-Smooth Dynamical Systems. Theory and Applications*. Series: Applied Mathematical Sciences, vol. 163. Springer, Berlin (2008).

[2] A.C.J.Luo, *Singularity and Dynamics on Discontinuous Vector Fields*. Monograph Series on Nonlinear Science and Complexity, vol. 3. Elsevier, Amsterdam (2006).

[3] J. Awrejcewicz, C.-H. Lamarque, *Bifurcation and Chaos in Nonsmooth Mechanical Systems*.World Scientific Series on Nonlinear Science: Series A, vol. 45. World Scientific Publishing, Singapore (2003).

[4] A.F. Filippov, *Differential Equations with Discontinuous Right-Hand Sides*. Kluwer Academic, Dordrecht (1988).

[5] W.J. Stronge, *Impact mechanics*. Cambridge University Press, Cambridge (2000).

[6] A. Mehta (ed.), *Granular Matter: An Interdisciplinary Approach*. Springer, Berlin (1994).

[7] C. Knudsen, R. Feldberg, H. True, Bifurcations and chaos in a model of a rolling wheel-set. Philos. Trans. R. Soc. Lond. A **338** (1992) 455–469.

[8] M. Wiercigroch, A.M. Krivtsov, J. Wojewoda, Vibrational energy transfer via modulated impacts for percussive drilling. Journal of Theoretical and Applied Mechanics **46** (2008) 715-726.

[9] A. C. J. Luo, Y. Guo, Motion Switching and Chaos of a Particle in a Generalized Fermi-Acceleration Oscillator, Mathematical Problems in Engineering, vol. **2009**, Article ID 298906, 40 pages, 2009. doi:10.1155/2009/298906.

[10] A. Okninski, B. Radziszewski, Dynamics of impacts with a table moving with piecewise constant velocity, Vibrations in Physical Systems, vol. XXIII, p.289 – 294, C. Cempel, M.W. Dobry (Editors), Poznań 2008.

[11] A. Okninski, B. Radziszewski, Dynamics of a material point colliding with a limiter moving with piecewise constant velocity, in: Modelling, Simulation and Control of Nonlinear Engineering Dynamical Systems. State-of-the Art, Perspectives and Applications, J. Awrejcewicz (Ed.), Springer 2009, pp. 117-127.

[12] A. Okninski, B. Radziszewski, Dynamics of impacts with a table moving with piecewise constant velocity, Nonlinear Dynamics **58** (2009) 515-523.

[13] A. Okninski, B. Radziszewski, Chaotic dynamics in a simple bouncing ball model, Proceedings of the 10th Conference on Dynamical Systems: Theory and Applications, December 7-10, 2009. Łódź, Poland, J. Awrejcewicz, M. Kazmierczak, P. Olejnik, J. Mrozowski (eds.), pp. 651-656.

[14] A. Okninski, B. Radziszewski, Chaotic dynamics in a simple bouncing ball model, arXiv:1002.2448 [nlin.CD] (2010), Acta Mechanica Sinica, to be published.

[15] A. Okninski, B. Radziszewski, Simple models of bouncing ball dynamics and their comparison, arXiv:1006.1236 [nlin.CD] (2010).

[16] A. Okninski, B. Radziszewski, Grazing dynamics and dependence on initial conditions in certain systems with impacts, arXiv:0706.0257 [nlin.CD] (2007).